

See discussions, stats, and author profiles for this publication at: <https://www.researchgate.net/publication/49807141>

# Osteogenic differentiation of human adipose-derived stem cells induced by osteoinductive calcium phosphate ceramics

ARTICLE in JOURNAL OF BIOMEDICAL MATERIALS RESEARCH PART B APPLIED BIOMATERIALS · APRIL 2011

Impact Factor: 2.76 · DOI: 10.1002/jbm.b.31773 · Source: PubMed

CITATIONS

49

READS

35

7 AUTHORS, INCLUDING:



**Xiaoming Li**

Beihang University(BUAA)

53 PUBLICATIONS 1,409 CITATIONS

SEE PROFILE



**Xufeng Niu**

Beihang University(BUAA)

39 PUBLICATIONS 669 CITATIONS

SEE PROFILE



**Qing Ling Feng**

Tsinghua University

205 PUBLICATIONS 5,905 CITATIONS

SEE PROFILE



**Fumio Watari**

Hokkaido University

256 PUBLICATIONS 5,176 CITATIONS

SEE PROFILE

# Osteogenic differentiation of human adipose-derived stem cells induced by osteoinductive calcium phosphate ceramics

Xiaoming Li,<sup>1</sup> Haifeng Liu,<sup>1</sup> Xufeng Niu,<sup>1</sup> Yubo Fan,<sup>1</sup> Qingling Feng,<sup>2</sup> Fu-zhai Cui,<sup>2</sup> Fumio Watari<sup>3</sup>

<sup>1</sup>Key Laboratory for Biomechanics and Mechanobiology of Ministry of Education, School of Biological Science and Medical Engineering, Beihang University, Beijing 100191, China

<sup>2</sup>Department of Materials Science and Engineering, Tsinghua University, Beijing 100084, China

<sup>3</sup>Department of Biomedical Materials and Engineering, Graduate School of Dental Medicine, Hokkaido University, Sapporo 060-8586, Japan

Received 30 July 2010; revised 28 September 2010; accepted 13 October 2010

Published online 2 February 2011 in Wiley Online Library (wileyonlinelibrary.com). DOI: 10.1002/jbm.b.31773

**Abstract:** Microstructure is indispensable for the osteoinduction of calcium phosphate ceramics. To study how microstructure takes its role and explore the mechanism of the osteoinduction, we evaluated attachment, proliferation, alkaline phosphatase (ALP)/DNA, protein/DNA, and mineralization of human adipose-derived stem cells cultured on two kinds of biphasic calcium phosphate (BCP) ceramic discs with the same chemistry and dimension, but different microporosity and surface area. BCP-A had been found osteoinductive *in vivo* while BCP-B was not. During the conventional culture, ALP/DNA and protein/DNA of the cell on BCP-A with larger surface area were significantly higher than those of the cells on BCP-B. With the adsorption of the proteins in culture medium with 50% fetal bovine serum (FBS) in advance, the increments of the ALP/DNA and protein/DNA for the BCP-A were found respectively significantly more than the increments of those for BCP-B, suggesting that the larger amount

of protein adsorbed on the BCP-A was crucial. More results showed that ALP/DNA and protein/DNA of the cells on the two kinds of discs presoaked in culture medium having additional rhBMP-2 were found to be both higher than those of the cells on the discs resoaked in culture medium with 50% FBS, and that those values for BCP-A increased much more. Furthermore, larger mineral content was found on BCP-A than on BCP-B at day 7. The results indicated that by increasing microporosity and thus surface areas, osteoinductive calcium phosphate ceramics concentrate more proteins, including bone-inducing proteins, and thereafter stimulate inducible cells in soft tissues to form inductive bone. © 2011 Wiley Periodicals, Inc. *J Biomed Mater Res Part B: Appl Biomater* 97B: 10–19, 2011.

**Key Words:** calcium phosphate, microporosity, osteogenic differentiation, protein adsorption

## INTRODUCTION

Because of their biocompatibility and bioactivity, calcium phosphate ceramics have been widely used as bone substitutes and dental devices for bone regeneration.<sup>1–10</sup> Despite their biocompatibility and bioactivity, calcium phosphate ceramics vary with their chemistry, macrostructures, microstructure, etc. Moreover calcium phosphate ceramics vary with their bone forming capacity. The bone forming ability of calcium phosphate ceramics varies in soft tissue.<sup>11–16</sup> Some calcium phosphate ceramics give rise to bone formation in soft tissues, thus becoming osteoinductive, while the others are not osteoinductive. So synthetic calcium phosphate ceramics without exogenous osteogenic and/or growth factors can be made osteoinductive by physicochemical modification of synthetics, while why and how materials induced ectopic bone formation are not known as yet.

A number of studies have concerned the short-term or long-term interactions of bone cells with calcium phosphate

ceramics.<sup>17–27</sup> The higher expression of bone-specific proteins like alkaline phosphatase (ALP) and osteocalcin on sintered HA than on brushite suggested that the composition of ceramics influences especially cell differentiation. Besides, calcium phosphate materials have been shown to have a very high adsorption capacity for serum proteins compared with other materials.<sup>22,28–31</sup> Fellah et al.<sup>32</sup> reported that bone could grow centripetally and progress toward the center of the defects after a bone substitute containing biphasic calcium phosphate (BCP) particles was rejected into the defect at the distal femoral epiphyses of New Zealand White rabbits for 8 weeks. Furthermore, mineralized and mature bone was observed between and in contact with the BCP particles, which showed that BCP particles supported the bone healing process. Schopper et al.<sup>33</sup> demonstrated abundant bone formation into the scaffolds and micromechanical interlocking at the bone/biomaterial interface without intervening soft tissue after a BCP biomaterial was implanted into corticocancellous

**Correspondence to:** X. Li; e-mail: x.m.li@hotmail.com or Y. Fan; e-mail: yubofan@buaa.edu.cn

Contract grant sponsor: National Natural Science Foundation of China; contract grant numbers: 31000431, 10925208, 50803032

Contract grant sponsor: Fundamental Research Funds for the Central Universities of China

Contract grant sponsor: Research Fund for the Doctoral Program of Higher Education of China; contract grant numbers: 2009110, 2110031

costal defects of sheep for 6 months. Mandubal et al.<sup>34</sup> reported the bone in-growth induced by BCP ceramic in the experimentally created circular defects in the femur of dogs. The defect was completely filled with new woven bone after 12 weeks, which proved that BCP could be made into osteoinductive biomaterials. So BCP ceramics with both HA and TCP appeared to have higher bone forming ability, and it has been shown that chemistry of calcium phosphate ceramics affected inductive bone formation in calcium phosphate ceramics.

However, to allow the inductive bone formation to occur in calcium phosphate ceramics, material composition is not the only qualification. Although with the same chemical composition, some materials are osteoinductive, some others are not. So, specific material properties are apparently needed for starting the process of bone induction. It has been suggested that the microenvironment around the cells may be crucial.<sup>4,35–37</sup> Barrere et al.<sup>38</sup> proposed that the microstructures of calcium phosphate biomaterials could influence their osteogenicity. Fujibayashi et al.<sup>39</sup> suggested that even a nonsoluble metal that contains no calcium or phosphorus can be an osteoinductive material when treated to form an appropriate microstructure. Kondo et al.<sup>40</sup> have shown that microstructures of  $\beta$ -TCP play an important role as the storage space for extracellular matrix components, including collagen, as well as providing ideal conditions for osteoinductivity. Yamasaki and Sakai<sup>10</sup> showed that after two HA ceramics, dense and porous, were implanted into nonosseous sites of dogs for 3 months, the micropores of the porous HA ceramics were found full of eosinophilic amorphous substance, suggesting a bone matrix; however, the dense HA ceramics were surrounded only by collagen fibres and occasional macrophages and multinucleated giant cells, no newly formed osseous tissue. Yuan et al.<sup>3</sup> showed that S-HA sintered at 1100°C is osteoinductive in dogs, but J-HA sintered at 1200°C with similar chemical compositions, crystallinities, and macrostructures, but much less micropores compared with S-HA is nonosteoinductive in the same animals.

Although the exact mechanism of the essential role of micropores in bone formation in calcium phosphate ceramics has not been found, some hypotheses could be found in former publications. The micropores might significantly increase the surface area of the material and this could enhance protein adsorption and cell adhesion on the biomaterials.<sup>4,14,15,41–43</sup> So, it was well admitted that the cellular response to a material should only be a secondary event. It was believed that a layer of adsorbed proteins should exist on the surface of all implant materials after immersion in biological fluids, and the presence of this preadsorbed protein layer might be essential in mediating cell response to the material.

In the current study, we evaluated human adipose-derived stem cells (HASCs) cultured on two kinds of BCP ceramic discs with the same chemistry and dimension but different microporosity and surface area. BCP-A had been found osteoinductive, while BCP-B was not. The purpose of the study was to gain insight into the mechanism underlying this difference in osteoinductive capacity of the microstructured calcium phosphate ceramics.

## MATERIALS AND METHODS

Two types of BCP discs namely, BCP-A and BCP-B, were prepared with H<sub>2</sub>O<sub>2</sub> method from calcium phosphate apatite powder with a Ca/P ratio of 1.61. Firstly, calcium phosphate apatite powder was mixed with diluted H<sub>2</sub>O<sub>2</sub> solution to get slurry that was subsequently put into moulds with the dimension of 3.0 cm in diameter and 1.6 cm in height to get cylinders. After foaming and drying at 60°C, the cylinders were sintered at 1150°C for 8 hours. Half of the cylinders sintered at 1150°C were machined to get the cylinders with the dimension of 10.0 ± 0.2 mm in diameter, and further cut with diamond saw to discs of 10.0 ± 0.2 mm in diameter and 1.00 ± 0.02 mm in height. BCP-A was finally obtained after the surface was polished with 4000# SiC paper and cleaned. The other half cylinders sintered at 1150°C was machined to cylinders with the diameter of 11.0 ± 0.2 mm and further cut to discs of 11.0 ± 0.2 mm in diameter and 1.10 ± 0.02 mm. After the surface was polished with 4000# SiC paper and cleaned, the discs were sintered again at 1300°C for 8 hours to get BCP-B with the dimension of 10.0 ± 0.2 mm in diameter and 1.00 ± 0.02 mm in height.

Chemical compositions and crystal structures of the ceramics were determined from Fourier transform infrared spectroscopy (FTIR; Spectrum100, PerkinElmer Analytical Instruments, Norwalk, CT) and X-ray diffraction (XRD; Miniflex, Rigaku, Japan). HA/b-TCP weight ratios in the BCP ceramics were determined by comparing the BCP XRD patterns to the calibration patterns prepared from the powders with the known HA/ $\beta$ -TCP weight ratios.

Microstructures of the porous BCP ceramics were characterized by scanning electron microscopy (SEM; S-4000, Hitachi, Japan). In addition, total microporosities (pore diameter <10  $\mu$ m) and average pore sizes and pore size distributions were determined using a mercury intrusion porosimeter (MP; Auto Pore IV 9500, Micromeritics European Analysis Service, Mönchengladbach, Germany). For comparison, the microporosity of each ceramic was expressed as total incremental pore volume (milliliter) per gram of the material for the pores with a diameter lower than 10  $\mu$ m. Specific surface areas of the ceramics were determined from the MP results as the cumulative surface area (square meter per gram) when all pores were filled with mercury. Specific surface area per disc (square meter) was figured out by the multiplication of the cumulative surface area and the weight of the disc.

Surface roughness of the discs was characterized with a UBM Microfocus Laser Profilometer (NanoFocus Inc., Sunnyvale, CA), which is composed of UBM measurement system, Microfocus Messsystem, and a personal computer in which specific software was installed. With the help of these apparatus, the surface profile can be scanned, and on the basis of this profile, various surface roughness parameters can be calculated according to DIN (Deutsches Institut für Normung) standards.

Before cells culture, ability to adsorb proteins of the discs was evaluated. At first, 0.25% FBS (250  $\mu$ L FBS in 100 mL

25 ppm  $\text{NaN}_3$  solution) was sterilized with 0.22- $\mu\text{m}$  filter. After immersing the compacts respectively for 1, 4, and 7 days, the residual protein content ( $\text{I}$ ) of the FBS solution (3 mL per sample,  $n = 5$ ) was determined with the QuantiPro™ BCA Assay Kit (TaKaRa BIO INC, Japan) according to the guideline of the company. The fluorescence was measured with a BIO-TEK automate microplate reader at 620 nm. The adsorbed protein ( $\text{a}$ ) was determined by the formula of  $(0.25\% - \text{I})/0.25\%$

HASCs were isolated from freshly excised human subcutaneous adipose tissue (donor age between 34 and 47 years) with approval of the Health Human Research Ethics Committee of Hebei Medical University. In brief, fat (300 mL) was minced into pieces (1 mm  $\times$  1 mm) and washed extensively with equal volumes of phosphate-buffered saline (PBS), and then incubated at 37°C for 45–60 min in 0.075% type I collagenase (Sigma). Enzyme activity was neutralized with Dulbecco's modified Eagle's medium-low glucose (DMEM-lg, Sigma), containing 10% fetal calf serum (FCS, Sigma) and cells were centrifuged at 1200 rpm for 10 min to remove adipocytes. The pellet was resuspended in 0.16 M  $\text{NH}_4\text{Cl}$  and incubated at room temperature for 5 min to lyse red blood cells. The cells were collected by centrifugation at 1200 rpm for 5 min, filtered through a 100- $\mu\text{m}$  nylon mesh to remove fissile debris, and incubated on culture plates overnight at 37°C in a humidified atmosphere containing 5%  $\text{CO}_2$  in control medium (DMEM-lg, 10% FCS, 1% antibiotic/antimycotic solution). Following incubation, the plates were washed extensively with PBS to remove residual non-adherent cells.

For the cell seeding on the disc, the culture medium was  $\alpha$ -minimum essential medium ( $\alpha$ -MEM; Sigma) containing 10% fetal bovine serum (FBS; Biowest), antibiotics, 0.2 mM ascorbic acid 2-phosphate, basic fibroblast growth factor, and  $10^{-8}$  dexamethasone (Dex; Sigma).

The cells (passage 2) were respectively seeded on the BCP discs placed in 25-well plates with a cell density of  $2.0 \times 10^4$  per sample by pipetting the cell suspension simply onto the surface. Then the samples were put into an incubator at 37°C in a humidified atmosphere with 5%  $\text{CO}_2$  and 95% air for 4 hours. Finally, 3 mL culture medium was added into the wells of the plates and then, the plates were put back to the incubator. The culture mediums were refreshed twice a week.

At the prescribed time, the samples were rinsed with PBS to remove non-adherent cells, fixed in a solution of 2% glutaraldehyde, and post-fixed in a 1% osmium tetroxide solution. Then, the samples were dehydrated in a series of solutions with increasing ethanol concentrations, followed by critical-point drying at 40°C. Finally, the morphology of the cells on the compacts was examined by scanning electron microscopy (SEM; S-4000, Hitachi, Japan).

Cells on the discs after cultured for 1, 4, 7, 14 days were evaluated by biochemical analyses including DNA, ALP, and protein analysis. Firstly, the discs with cells were washed by PBS for three times after the cultured medium

was totally removed. Then the samples were stored in the freezer at  $-80^\circ\text{C}$  for at least 12 hours for the biochemical analyses. As soon as the plates were taken out from the freezer, they were kept on the ice, prepared in advance. And then 0.5 mL 0.2% triton was put into each well with samples in the plates. The plates were shaken gently for 45 min. Finally, the triton solutions with lysed cells were analyzed for DNA, ALP, and protein content. DNA content was mensurated with the CyQuant Cell Proliferation Assay Kit (Sigma, The Netherlands). Fifty microlitres of each sample ( $n = 4$ ) was added to the wells of a 96-well plate. Then 50  $\mu\text{L}$  of lysis buffer 1X (lysis buffer 20 $\times$  was diluted in the solution of 180 mM NaCl, 1 mM EDTA, and 1.35 Kunitz Rnase A/mL; lysis buffer 20 $\times$  NaCl, EDTA, and Kunitz Rnase were from Sigma, the Netherlands) was added to the plate. After the plate was continuously shaken in dark at room temperature for 1 hour, 100  $\mu\text{L}$  Cyquant GRDye was added to each sample. After the plate was continuously shaken in dark at room temperature for 15 min, the fluorescence using a fluorimeter (PerkinElmer) was measured at an emission wavelength of 520 nm and excitation of 480 nm. The DNA content of cells attached on the porous samples was counted through a premade standard DNA curve. DNA content was expressed as mean  $\pm$  SD. For the determination of ALP content, 100  $\mu\text{L}$  of each sample ( $n = 4$ ) was added to the wells of a 96-well plate, and then 100  $\mu\text{L}$  Paranitrophenyl phosphate (PNP; Sigma, The Netherlands) solution was added. After shaking gently, the plate was put into 37°C incubator in dark. After 2 hours, the plate was read with a BIO-TEK automate microplate reader at 405 nm. For the standard curve, serial dilutions of 4-nitrophenol were made. Finally, the ALP content of cells was counted through the standard curve. The value was expressed as mean  $\pm$  SD. Protein content was mensurated with the QuantiPro™ BCA Assay Kit (Sigma, The Netherlands). First 100  $\mu\text{L}$  of each sample ( $n = 4$ ) was added to the wells of a 96-well and then 100  $\mu\text{L}$  BCA solution was added. Then, the plate was continuously shaken for 2 hours in dark at room temperature. Finally, the fluorescence was measured with a BIO-TEK automate microplate reader at 620 nm. The protein content, expressed as mean  $\pm$  SD, was counted through a premade standard protein curve.

At first, the discs were respectively immersed into culture medium containing 50% FBS for 24 hours in an incubator at 37°C in a humidified atmosphere with 5%  $\text{CO}_2$  and 95% air. Then, the FBS solution was completely removed and the discs were washed by the cultured medium of the HASCs cells with 1% FBS for three times. The HASCs cells were respectively cultured on the samples with a cell density of  $4.0 \times 10^4$  per sample. After cell culture in culture medium with 1% FBS for 4 days and 7 days, DNA, ALP, total protein content, and mineralized modules were examined with the methods mentioned above.

At first, the samples were respectively immersed in rhBMP-2 (Yamanouchi Pharmaceutical Co. Ltd., Tokyo, Japan) solutions

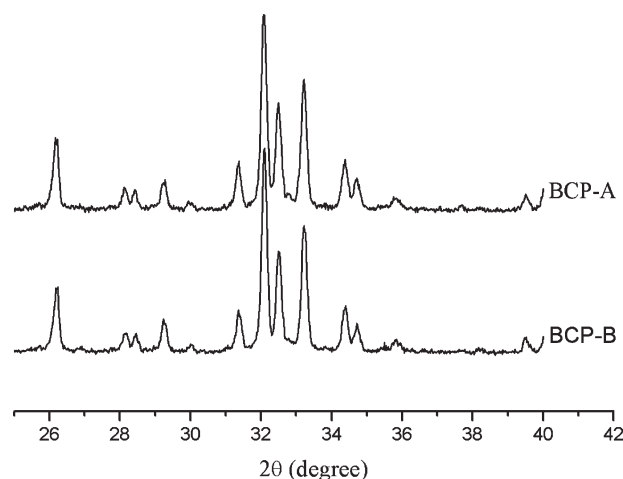


**FIGURE 1.** XRD pattern of BCP discs.

(rhBMP-2 in the cell culture medium) with concentration of 500 ng/mL for 24 hours in an incubator at 37°C in a humidified atmosphere with 5% CO<sub>2</sub> and 95% air. Then, the solution was completely removed and the samples were washed by the cultured medium of the HASCs with 1% FBS three times. And then, the cells were respectively cultured on the samples with a cell density of  $5.0 \times 10^4$  per sample. After cell culture in culture medium with 1% FBS for 4 days and 7 days, DNA, ALP, total protein content, and mineralized modules were examined with the methods mentioned above.

Xylenol orange (XO), a nontoxic fluorochrome chelating reagent that labels newly calcified tissues,<sup>44</sup> was used to nondestructively visualize mineralized modules in the cell cultures at 7 days. XO powder (Sigma) was dissolved in distilled water and filtered to make a concentrated 20 m stock and stored at 4°C. XO was added to the culture medium at a final concentration of 20  $\mu$  at least 12 hours before imaging. XO-containing medium was exchanged for fresh medium prior to imaging to avoid the nonspecific fluorescent background. The images were collected on a

fluorescence microscope (Eclipse TE 300, Nikon Inc.). The fluorescence intensity of the XO stained mineral was quantified with a fluorometer (Safire II, Tecan) with 546 nm excitation, 580 nm emission, and 10 nm bandwidth.

Obtained data were statistically analyzed with one-way ANOVA, followed by a Tukey's post hoc test (SPSS Inc., Chicago, IL, USA). A  $p < 0.05$  was regarded as significant difference.

## RESULTS

XRD patterns of the two ceramics are given in Figure 1. Both kinds of BCP ceramics had similar, biphasic structure, consisting of HA and  $\beta$ -TCP. All ceramics were fully crystalline and consisted of  $80 \pm 3$  wt % HA and  $20 \pm 3$  wt %  $\beta$ -TCP.

The microstructures of the two kinds of discs were different. Changes of the sintering temperature or adding pressing method changed the materials' microstructures. The SEM of the two kinds of discs showed that the microspore number of BCP-A was significantly more than that of BCP-B (Figure 2). In addition, the mercury intrusion results showed the micropore size distribution, porosity (Figure 3). Most micropores of BCP-A had a diameter of around 1.2  $\mu$ m, whereas the diameters of the BCP-B were respectively 1.5  $\mu$ m. The total incremental volume of micropores (microporosity) was much higher for BCP-A (about 49.6%) as compared with BCP-B (25.8%). At last, the micropore properties were summarized by specific surface areas (Table I). The specific surface area of BCP-A was much higher than that of BCP-B, which is the result of the combination of micropore size and microporosity.

On the other hand, the surface roughness of BCP-B was significantly bigger than that of BCP-A (Table II).

Moreover, the ability of protein adsorption of the discs is shown in Figure 4, which showed that BCP-A had much bigger ability of protein than BCP-B. This result confirmed

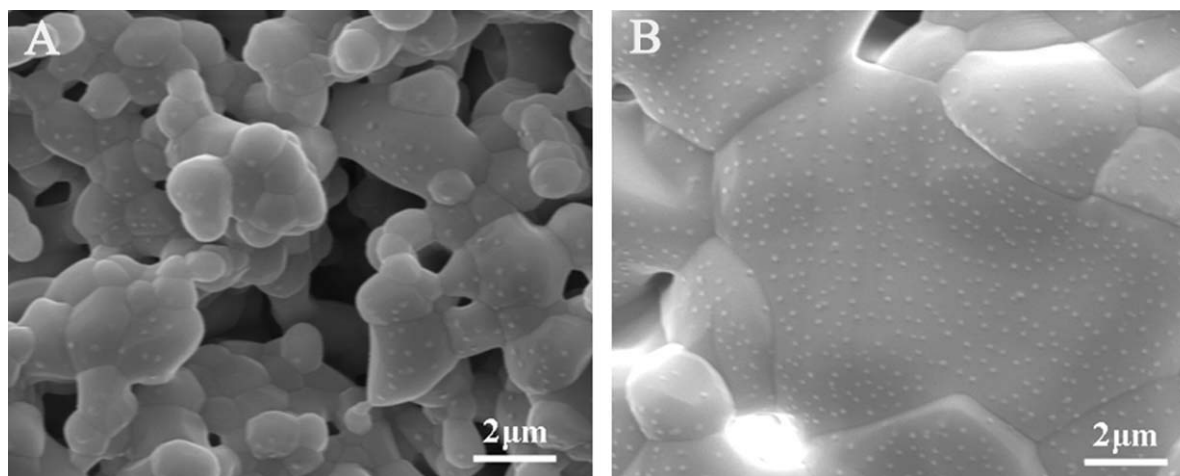


**FIGURE 2.** SEM of (A) BCP-A and (B) BCP-B, showing BCP-A has more microspores than BCP-B.



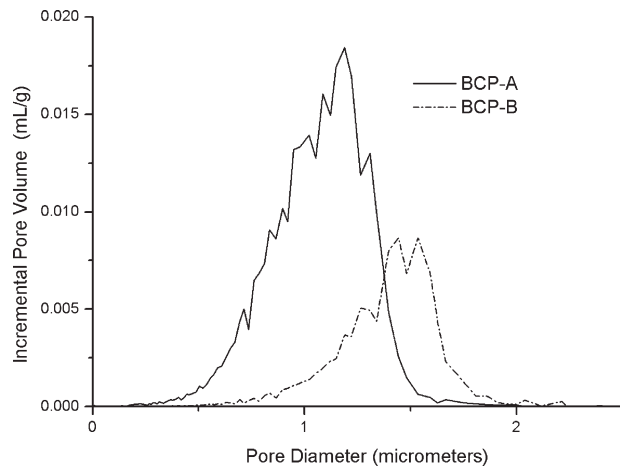


**FIGURE 3.** Total incremental micropore volume for the two kinds of BCP discs. BCP-A has much bigger microporosity than BCP-B.

the fact of the bigger specific surface area, the higher ability of protein adsorption.

Morphology of the cells cultured at 4 hours after seeding on the two kinds of discs is shown in Figure 5, which showed that the HASCs attached better on BCP-B than on BCP-A. The results of DNA analysis showed that there was no significant difference in the cell proliferation (slope of the two curves from day 1 to day 4:  $1.258 \pm 0.052$  vs.  $1.219 \pm 0.086$ ,  $> 0.05$ ; from day 4 to day 7:  $0.568 \pm 0.021$  vs.  $0.563 \pm 0.082$ ,  $> 0.05$ ; from day 7 to day 14:  $0.461 \pm 0.066$  vs.  $0.489 \pm 0.036$ ,  $> 0.05$ ) on the two kinds of discs (Figure 6).

Figure 7 shows the results of ALP/DNA, alkaline phosphatase per unit cell, of the cells on the BCP discs. ALP/DNA of the HASCs cultured on BCP-A was significantly higher than that on BCP-B at each culture time point of 1, 4, 7 and 14 days ( $< 0.05$ ), showing that HASCs differentiate toward osteogenic better on BCP-A than on BCP-B.

Figure 8 shows the results of protein/DNA, total protein content per unit cell, of the cells on the BCP discs. Protein/DNA of all the cells cultured on BCP-A was significantly higher than that on BCP-B at each culture time point of 1, 4, 7 and 14 days ( $< 0.05$ ), showing that the cells on BCP-A were more active than those on BCP-B.

Figure 9 shows ALP/DNA of the cells on the samples after adsorbing FBS at day 4 and day 7, comparing with the results of the conventional cell culture. After the adsorption

**TABLE I. Specific Surface Area and Microporosity of the BCP Discs**

BCP Discs	Specific Surface Area ( $\text{m}^2/\text{g}$ )	Specific Surface Area Per Disc ( $\text{m}^2$ ) ( $n = 5$ )	Microporosity (%)
BCP-A	1.205	$0.180 \pm 0.008$	49.6
BCP-B	0.839	$0.062 \pm 0.006$	25.8

**TABLE II. Surface Roughness of the BCP Discs**

BCP Discs	Average Surface Roughness ( $R_a$ ; $\mu\text{m}$ ) ( $n = 8$ )
BCP-A	$0.68 \pm 0.19$
BCP-B	$3.16 \pm 1.31$

of FBS, ALP/DNA of cells on the BCP-A increased significantly, while the value for BCP-B increased slightly. The increased value for the BCP-A was as about four times as that for BCP-B at both day 4 and day 7.

Protein/DNA of the cells on the samples after adsorbing FBS on day 4 and day 7, comparing with the results of the conventional cell culture, is shown in Figure 10. Although the protein/DNA of cells on all the samples all increased after the adsorption of FBS, the value for the BCP-A increased most observably ( $< 0.05$ ). The increased value for the BCP-A was as about 2.5 times as that for BCP-B on both day 4 and day 7.

Figure 11 shows that ALP/DNA of the cells on the samples all increased after adsorbing rhBMP-2 at day 4 and day 7, compared with the results of the cell culture on the discs after adsorbing FBS. However, ALP/DNA of cells on the BCP-A increased more ( $< 0.05$ ). The increased value for the BCP-A was as about 4.5 and 5.5 times as that for BCP-B on day 4 and day 7, respectively.

Protein/DNA of the cells on the samples all increased after adsorbing rhBMP-2 on day 4 and day 7, comparing with the results of the cell culture on the discs after adsorbing FBS, is shown in Figure 12. The value for the BCP-A increased more significantly ( $< 0.05$ ). The increased value for the BCP-A was as about 2.5 and 3 times as that for BCP-B on day 4 and day 7, respectively.

Mineral content was visualized after XO staining by microscopy, and the fluorescence intensity was quantified

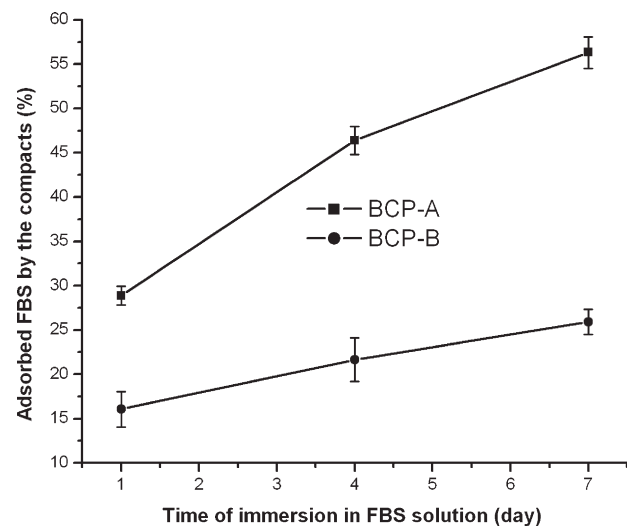


**FIGURE 4.** Ability of protein adsorption of the BCP discs ( $n = 5$ ), indicating the protein adsorption ability of BCP-A is much bigger than that of BCP-B.

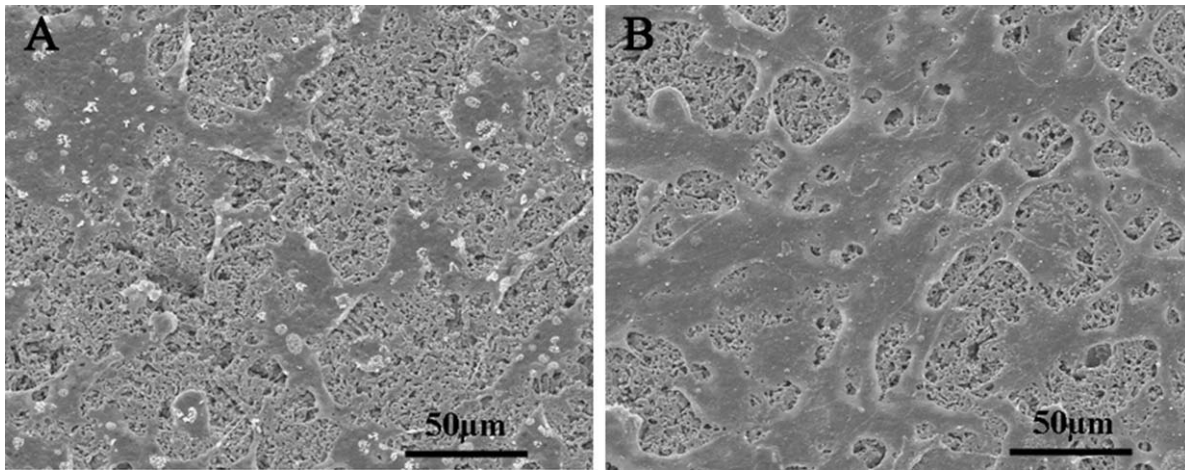


**FIGURE 5.** SEM images of the cells cultured at 4 hours after seeding on (A) BCP-A and (B) BCP-B, showing that the HASCs attached better on BCP-B than on BCP-A

by fluorimetry at day 7. On the BCP-A surface, larger area of continuous XO staining was displayed (Figure 13). The area of XO staining quantified by image analysis was sevenfold higher on BCP-A than on BCP-B and was highly statistically significantly different ( $p < 0.01$ ). The biomaterial background was subtracted. This result further indicated that the cells on BCP-A differentiated into osteogenic cells better than on BCP-B.

## DISCUSSION

Osteoinduction by calcium phosphate biomaterials in various forms has been shown in various reports in the last decade, as was shown in introduction part. However, so far, the acknowledged mechanism of the phenomenon underlying the osteoinduction is still lacking. The main purpose of our present study was to find out the mechanisms of osteoinduction, at least to add to the knowledge of parameters that

influence calcium phosphate material osteoinductive properties. Cells in their natural environment interact with extracellular matrix (ECM) components in the micrometer scale. Logically, the microstructures of biomaterials should have effect on the cell functions. It has been indicated that the differentiation of the inducible cells into bone-forming cells is determined not only by their chemistry, but also by the level of micropore properties within the calcium phosphate ceramics, which directly determine their microstructures.<sup>5,12,45</sup> In this study, we compared the response of human adipose-derived stem cells cultured on osteoinductive and nonosteoinductive BCP ceramics, which had different micropore size and microporosity to find out how the micropores take their roles to differentiate the cells derived from soft tissue into osteogenic cells. Before the cell culture, we did a preliminary test, which showed that the degradation of the discs, put in the culture medium for 14 days, did not happen. So there was no effect of the material degradation on the cell culture in this study.

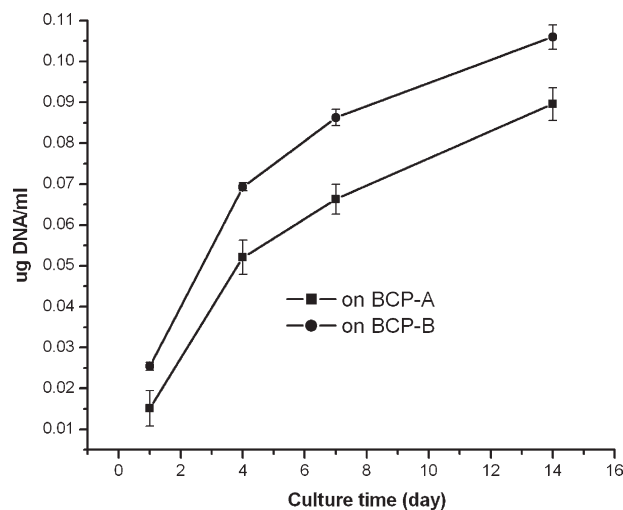


**FIGURE 6.** Results of DNA analysis of the HASCs cultured on BCP discs ( $n = 4$ ), showing there is no significant difference in their proliferation on the two kinds of discs (no significant difference in the slope of the curves,  $p > 0.05$ ).

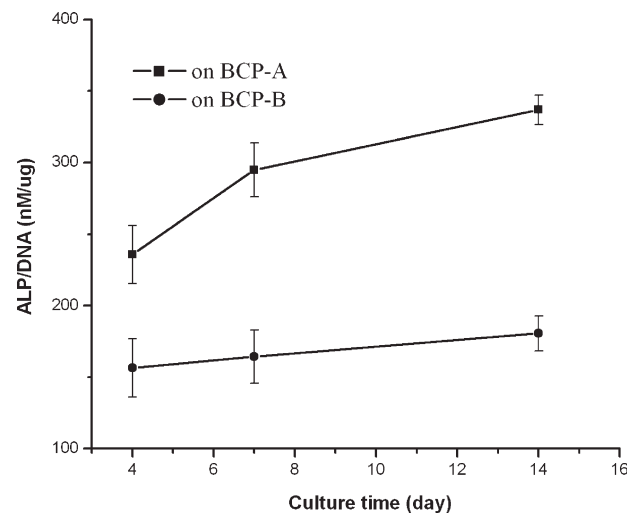


**FIGURE 7.** ALP/DNA of the HASCs cultured on BCP discs ( $n = 4$ ), showing that ALP/DNA of the cells on BCP-A is much bigger than on BCP-B.

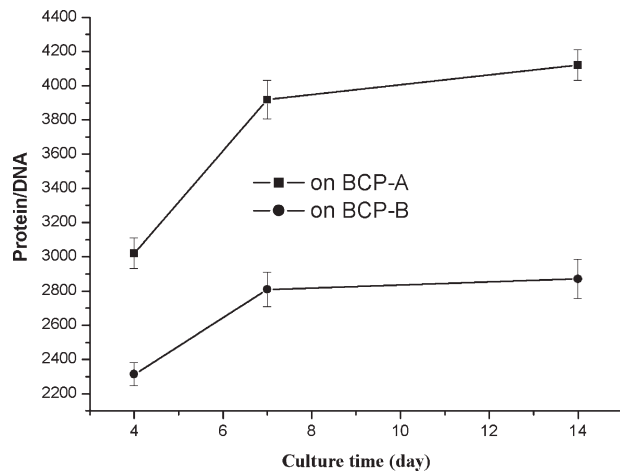


**FIGURE 8.** Protein/DNA of the HASCs cultured on BCP discs ( $n = 4$ ), showing that protein/DNA of the cells on BCP-A is much bigger than on BCP-B.

From the results of this study, we can see that the attachment of the cells on the BCP-B was better than on the BCP-A. Since the surface roughness of the BCP-B was bigger than that of BCP-A, the surface roughness might benefit the cell attachment. Another hypothesis is that surface area might influence cells attachment through concentrating some proteins from culture mediums. BCP may concentrate some specific proteins, which are not in favor of the cell attachment. Kilpadi et al.<sup>20</sup> found that some specific proteins have different influence on human marrow stromal cells attachment and saos-2 osteosarcoma cells attachments on hydroxylapatite. Since the cells attached better on the nonosteoinductive materials than on osteoinductive materials, cell attachment might not be one of the main qualifications for the inductive bone formation. Cell proliferation in this study might be mainly influenced by the chemistry. There is no significant difference in the cell proliferation on the two kinds of BCP discs, for they have the same chemical composition.

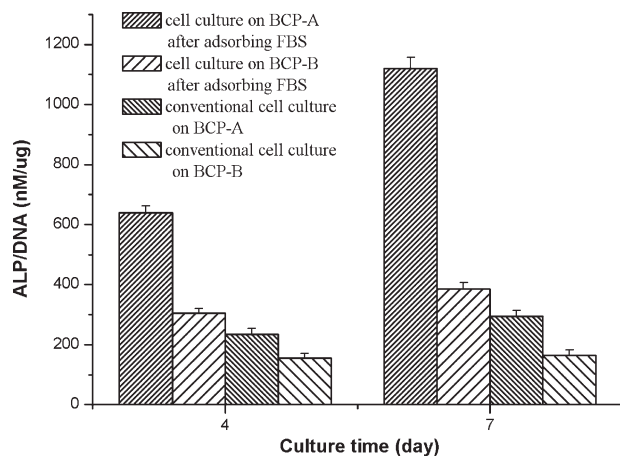


**FIGURE 9.** ALP/DNA of the HASCs cultured on the discs with and without the adsorption of FBS in advance ( $n = 4$ ), showing that after the adsorption of FBS, ALP/DNA of the cells on the two kinds of discs all increased, and that the value for BCP-A increased much more significantly.

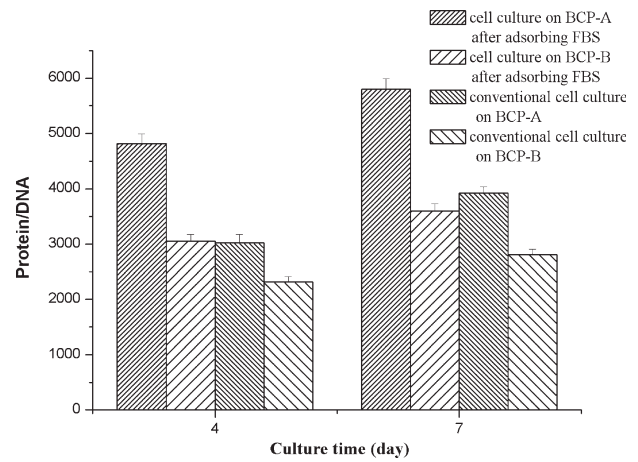


**FIGURE 10.** Protein/DNA of the HASCs cultured on the discs with and without the adsorption of FBS in advance ( $n = 4$ ), showing that after the adsorption of FBS, protein/DNA of the cells on the two kinds of discs all increased, and that the value for BCP-A increased much more significantly.

Besides cell attachment and proliferation, cell differentiation should be the most important evaluation point for biomaterials because it may directly contribute to the tissue repair.<sup>35</sup> The results of ALP/DNA and protein/DNA are most important and interesting in this study because they may have direct relations with the inductive bone formation. Alkaline phosphatase (ALP), a noncollagenous protein, is to be a potent inducer of bone formation and a highly specific marker of bone formation and osteoblast function of interest to clinicians and bone biologists because it is easy to measure and is useful as a significant predictor of osteogenic cells formation.<sup>46-49</sup> In this study, we used ALP/DNA to express the ALP activity per cell, thereby to characterize the ability of bone formation of each cell. Furthermore, besides ALP, there may be some others proteins, which may

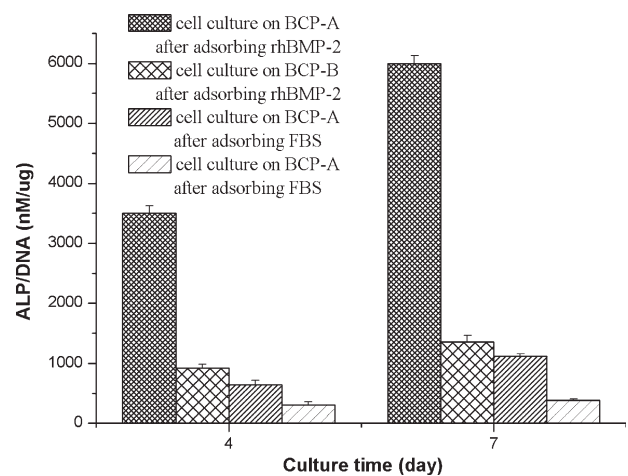


**FIGURE 11.** ALP/DNA of the HASCs cultured on the discs with the adsorption of FBS and rhBMP-2 in advance respectively ( $n = 4$ ), showing that comparing with the results of the cell culture on the discs after adsorbing FBS, ALP/DNA of the cells on the discs all increased after adsorbing rhBMP-2 at day 4 and day 7, and that the value for BCP-A increased much more significantly.



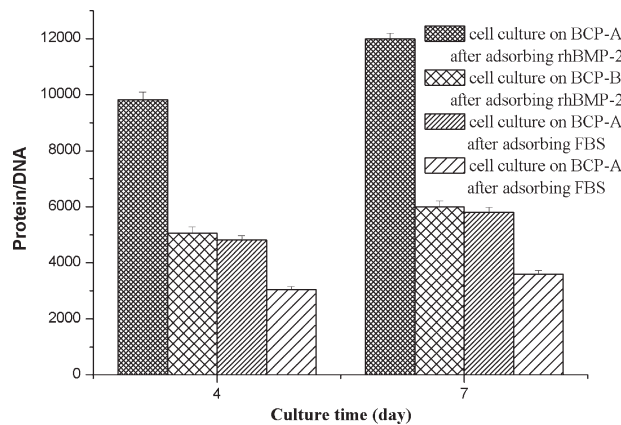


**FIGURE 12.** Protein/DNA of the HASCs cultured on the discs with the adsorption of FBS and rhBMP-2 in advance respectively ( $n = 4$ ), showing that comparing with the results of the cell culture on the discs after adsorbing FBS, protein/DNA of the cells on the discs all increased after adsorbing rhBMP-2 at day 4 and day 7, and that the value for BCP-A increased much more significantly.

be inducers of bone formation.<sup>50–53</sup> So, in our study, protein/DNA was used as an additional marker of cell activity for possible bone formation. The technique we used in this study for lysing cells before ALP, DNA, and protein analyses has been confirmed that only cells, no adsorbed proteins, could be lysed from the samples in advance. The results of the conventional cell culture showed that the ALP/DNA and the total-protein/DNA of the cells on BCP-A were both significantly higher than those on BCP-B, suggesting that BCP-A induce this kind of cell to differentiate into osteogenic cells better than BCP-B and that the cells on BCP-A were more active. We think that this was probably because BCP-A, with larger surface areas and bigger ability in protein adsorption, had adsorbed more proteins from culture medium than BCP-B, and these proteins made the cells differentiate to osteogenic cells. To confirm this hypothesis, we

immersed the samples in culture medium containing 50% FBS to make them adsorb more proteins before cell culture. The results showed that after the adsorption of FBS, both the total-protein/DNA and ALP/DNA increased on all samples. Impressively, the value for BCP-A increased most significantly. Therefore, the results of cell culture after the adsorption of FBS might be an effective proof for our hypothesis. Although BCP-A had bigger ability in protein adsorption, the species of protein adsorbed should be important for the inductive bone formation. Hing<sup>54</sup> has reported that competitive protein adsorption at a bioactive surface may vary in three ways: (i) the quantity of protein adsorbed, (ii) the species of protein adsorbed, or (iii) the confirmation of the adsorbed protein. Also he supposed that nanostructures might thus influence protein adsorption by providing a larger surface area, thereby increasing the quantity of adsorbed growth factors above a critical level for cell activation. To confirm the further hypothesis that the larger amount of specific proteins included in the adsorbed protein on BCP-A was indispensable in this osteogenic differentiation, we used BMP-2 as a specific growth factor and made the discs adsorb as much this specific growth factor as possible before cell cultures. The results, as we had speculated, showed that ALP/DNA and protein/DNA of the cells cultured on the two kinds of discs all increased after the adsorption of rhBMP-2 than after the adsorption of the FBS; furthermore, the values for BCP-A both increased most. In a previous study, Li. et al.<sup>35,55</sup> confirmed that the carbon nanotubes could induce cellular functions of C2C12 by adsorbing more proteins through making the samples adsorb more proteins in culture medium with 50% FBS before cell culture.

So, after the cells culture with the adsorption of FBS and rhBMP-2 (a kind of specific growth factor), we concluded that that increasing surface areas, microstructured calcium phosphate materials might concentrate more proteins, including bone-inducing proteins, and these proteins

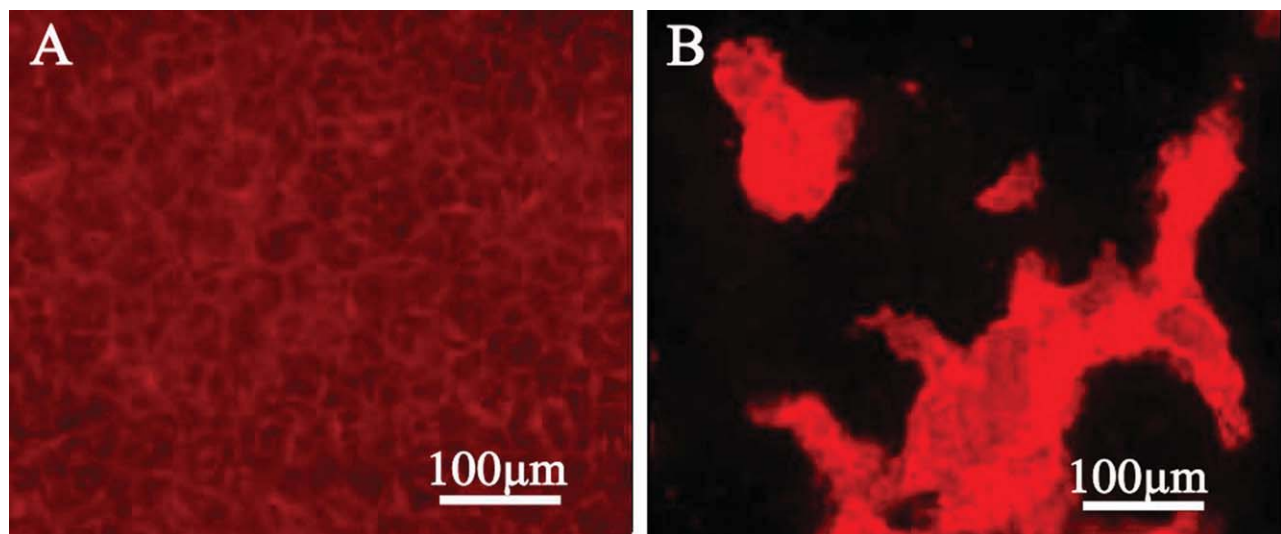


**FIGURE 13.** Fluorescent images of XO-stained mineral after 7 days culture on the BCP discs. On the BCP-A surface, larger area of continuous XO staining was displayed. [Color figure can be viewed in the online issue, which is available at [wileyonlinelibrary.com](http://wileyonlinelibrary.com).]

differentiated the cells derived from soft tissues to osteogenic cells, which formed inductive bone. In our study, we reified the importance of the protein adsorption. Though the specific proteins, adsorbed at surface of calcium phosphate, might be not helpful for cell attachment and proliferation, they could promote some inducible cells to differentiate to osteogenic cells. Philosophy tells us that everything has properties of two sides, which seems to be shown in this study. But we grasped the main side, for the differentiation of inducible cells to osteogenic cells is directly helpful for bone formation. Our findings may well provide answer or proofs for the hypothesis or make connection with the findings in the previous publications. Habibovic et al. and Li et al.<sup>4,51,56</sup> reported that BCP-A is osteoinductive and BCP-B is nonosteoinductive in goats and gave a hypothesis that the presence of micropores, the presence of which suggests a larger surface area, is necessary to make a material osteoinductive. Ripamonti et al. and Kuboki et al.<sup>57-59</sup> demonstrated that osteoinductivity in HA was linked to the precise shape of surface concavities in implants, which indicated a larger surface area.

## CONCLUSIONS

By increasing microporosity and thereafter surface areas, microstructured calcium phosphate ceramics concentrate higher amount of proteins, including bone-inducing proteins, which could differentiate inducible cells in soft tissues to osteogenic cells, to at the end improve bone forming ability, become osteoinductive in non-osseous sites.

## REFERENCES

- Li XM, Feng QL, Liu XH, Dong W, Cui FZ. Collagen-based implants reinforced by chitin fibres in a goat shank bone defect model. *Biomaterials* 2006;27:1917-1923.
- Yang Z, Yuan H, Tong W, Zou P, Chen W, Zhang X. Osteogenesis in extraskeletally implanted porous calcium phosphate ceramics: Variability among different kinds of animals. *Biomaterials* 1996; 17:2131-2137.
- Yuan H, Kurashina K, de Bruijn JD, Li Y, de Groot K, Zhang X. A preliminary study on osteoinduction of two kinds of calcium phosphate ceramics. *Biomaterials* 1999;20:1799-1806.
- Habibovic P, Yuan H, van der Valk CM, Meijer G, van Blitterswijk CA, de Groot K. 3D microenvironment as essential element for osteoinduction by biomaterials. *Biomaterials* 2005;26:3565-3575.
- Klein C, de Groot K, Chen WQ, Li YB, Zhang XD. Osseous substance formation induced in porous calcium phosphate ceramics in soft tissues. *Biomaterials* 1994;15:31-34.
- Ripamonti U. The morphogenesis of bone in replicas of porous hydroxyapatite obtained from conversion of calcium carbonate exoskeletons of coral. *J Bone Joint Surg Am* 1991;73:692-703.
- Hing KA, Annaz B, Saeed S, Revell PA, Buckland T. Microporosity enhances bioactivity of synthetic bone graft substitutes. *J Mater Sci Mater Med* 2005;16:467-475.
- Vargervik K. Critical sites for new bone formation. In: Habal MB, Reddi AH, editors. *Bone Grafts and Bone Substitutes*. Philadelphia, PA: WB Saunders; 1992. p 108.
- Yamasaki H. Heterotopic bone formation around porous hydroxyapatite ceramics in the subcutis of dogs. *Jpn J Oral Biol* 1990;32: 190-192.
- Yamasaki H, Sakai H. Osteogenic response to porous hydroxyapatite ceramics under the skin of dogs. *Biomaterials* 1992;13:308-312.
- Zhang X. A study of porous block HA ceramics and its osteogenesis. In: Ravaglioli A, Krajewski A, editors. *Bioceramics and the Human Body*. Amsterdam, The Netherlands: Elsevier Science; 1991. p 11.
- Gosain AK, Riordan PA, Song LS, Amarante MT, Kalantarian B, Nagy PG, Wilson CR, Toth JM, McIntyre BL. A 1-year study of osteoinduction in hydroxyapatite-derived biomaterials in an adult sheep model. Part II. Bioengineering implants to optimize bone replacement in reconstruction of cranial defects. *Plast Reconstr Surg* 2004;114:1155-1163.
- Gosain AF, Song LS, Riordan P, Amarante MT, Nagy PG, Wilson CR, Toth JM, Ricci JL. A 1-year study of osteoinduction in hydroxyapatite-derived biomaterials in an adult sheep model. Part I. *Plast Reconstr Surg* 2002;109:619-630.
- Habibovic P, Li JP, van der Valk CM, Meijer G, Layrolle P, van Blitterswijk CA, de Groot K. Biological performance of uncoated and octacalcium phosphate-coated Ti6Al4V. *Biomaterials* 2005;26: 23-36.
- Habibovic P, Van der Valk CM, Van Blitterswijk CA, De Groot K, Meijer G. Influence of octacalcium phosphate coating on osteoinductive properties of biomaterials. *J Mater Sci Mater Med* 2004; 15:373-380.
- Barrere F, van der Valk CM, Dalmeijer RAJ, Meijer G, van Blitterswijk CA, de Groot K, Layrolle P. Osteogenicity of octacalcium phosphate coatings applied on porous metal implants. *J Biomed Mater Res A* 2003;66:779-788.
- El-Ghannam A, Ducheyne P, Shapiro IM. Effect of serum proteins on osteoblast adhesion to surface-modified bioactive glass and hydroxyapatite. *J Orthop Res* 1999;17:340-345.
- Kilpadi KL, Chang PL, Bellis SL. Hydroxylapatite binds more serum proteins, purified integrins, and osteoblast precursor cells than titanium or steel. *J Biomed Mater Res* 2001;57:258-267.
- Wang CY, Duan YR, Markovic B, Barbara J, Howlett CR, Zhang XD, Zreiqat H. Phenotypic expression of bone-related genes in osteoblasts grown on calcium phosphate ceramics with different phase compositions. *Biomaterials* 2004;25:2507-2514.
- Kilpadi KL, Sawyer AA, Prince CW, Chang PL, Bellis SL. Primary human marrow stromal cells and SaOs-2 osteosarcoma cells use different mechanisms to adhere to hydroxylapatite. *J Biomed Mater Res A* 2003;68A:273-285.
- Sawyer AA, Hennessy KM, Bellis SL. Regulation of mesenchymal stem cell attachment and spreading on hydroxyapatite by RGD peptides and adsorbed serum proteins. *Biomaterials* 2005;26:1467-1475.
- Villareal DR, Sogal A, Ong JL. Protein adsorption and osteoblast responses to different calcium phosphate surfaces. *J Oral Implantol* 1998;24:67-73.
- Wang C, Duan Y, Markovic B, Barbara J, Howlett CR, Zhang X, Zreiqat H. Proliferation and bone-related gene expression of osteoblasts grown on hydroxyapatite ceramics sintered at different temperature. *Biomaterials* 2004;25:2949-2956.
- Webster TJ, Siegel RW, Bizios R. Osteoblast adhesion on nanophase ceramics. *Biomaterials* 1999;20:1221-1227.
- Webster TJ, Ergun C, Doremus RH, Siegel RW, Bizios R. Specific proteins mediate enhanced osteoblast adhesion on nanophase ceramics. *J Biomed Mater Res* 2000;51:475-483.
- Webster TJ, Massa-Schlueter EA, Smith JL, Slamovich EB. Osteoblast response to hydroxyapatite doped with divalent and trivalent cations. *Biomaterials* 2004;25:2111-2121.
- Rosa AL, Beloti MM, Van Noort R. Osteoblastic differentiation of cultured rat bone marrow cells on hydroxyapatite with different topography. *Dent Mater* 2003;19:768-772.
- Rosengren A, Pavlovic E, Oscarsson S, Krajewski A, Ravaglioli A, Piancastelli A. Plasma protein adsorption pattern on characterized ceramic biomaterials. *Biomaterials* 2002;23:1237-1247.
- Hughes Wassell DT, Hall RC, Embury G. Adsorption of bovine serum albumin onto hydroxyapatite. *Biomaterials* 1995;16:697-702.
- Takemoto S, Kusudo Y, Tsuru K, Hayakawa S, Osaka A, Takashima S. Selective protein adsorption and blood compatibility of hydroxycarbonate apatites. *J Biomed Mater Res A* 2004;69:544-551.
- Zheng H, Chittur KK, Lacefield WR. Analysis of bovine serum albumin adsorption on calcium phosphate and titanium surfaces. *Biomaterials* 1999;20:377-384.
- Fellah BH, Weiss P, Gauthier O, Rouillon T, Pilet P, Daculsi G, Layrolle P. Bone repair using a new injectable self-crosslinkable bone substitute. *J Orthop Res* 2006;24:628-635.
- Schopper C, Ziya-Ghazvini F, Goriwoda W, Moser D, Wanschitz F, Spassova E, Lagogiannis G, Auterith A, Ewers R. HA/TCP compounding of a porous CaP biomaterial improves bone

- formation and scaffold degradation—A long-term histological study. *J Biomed Mater Res B* 2005;74:458–467.
34. Mandubalal I, Sastry TP, Kumar RVS. Bone in-growth induced by biphasic calcium phosphate ceramic in femoral defect of dogs. *J Biomater Appl* 2005;19:341–360.
  35. Li XM, Gao H, Uo M, Sato Y, Akasaka T, Feng QL, Cui FZ, Liu XH, Watari F. Effect of carbon nanotubes on cellular functions *in vitro*. *J Biomed Mater Res A* 2009;91:132–139.
  36. Li XM, Gao H, Uo M, Sato Y, Akasaka T, Abe S, Feng QL, Cui FZ, Watari F. Maturation of osteoblast-like SaoS2 induced by carbon nanotubes. *Biomed Mater* 2009;4:015005.
  37. Li XM, Liu XH, Dong W, Feng QL, Cui FZ, Uo M, Akasaka T, Watari F. *In vitro* evaluation of porous poly (L-lactic acid) scaffold reinforced by chitin fibers. *J Biomed Mater Res B* 2009;90:503–509.
  38. Barrere F, van der Valk CM, Dalmeijer RAJ, Meijer G, van Blitterswijk CA, de Groot K, Layrolle P. Osteogenicity of octacalcium phosphate coatings applied on porous metal implants. *J Biomed Mater Res A* 2003;66:779–788.
  39. Fujibayashi S, Neo M, Kim HM, Kokubo T, Nakamura T. Osteoinduction of bioactive titanium metal. *Key Eng Mater* 2004;254–256: 953–956.
  40. Kondo N, Ogose A, Tokunaga K, Umezue H, Arai K, Kudo N, Hoshino M, Inoue H, Irie H, Kuroda K, Mera H, Endo N. Osteoinduction with highly purified beta-tricalcium phosphate in dog dorsal muscles and the proliferation of osteoclasts before heterotopic bone formation. *Biomaterials* 2006;27:4419–4427.
  41. De Groot J. Carriers that concentrate native bone morphogenetic protein *in vivo*. *Tissue Eng* 1998;4:337–341.
  42. Takemoto M, Fujibayashi S, Neo M, Suzuki J, Matsushita T, Kokubo T, Nakamura T. Osteoinductive porous titanium implants: Effect of sodium removal by dilute HCl treatment. *Biomaterials* 2006;27:2682–2691.
  43. Le Nihouannen D, Daculsi G, Saffarzadeh A, Gauthier O, Delplace S, Pilet P, Layrolle P. Ectopic bone formation by microporous calcium phosphate ceramic particles in sheep muscles. *Bone* 2005; 36:1086–1093.
  44. Wang YH, Liu Y, Buhl K, Rowe DW. Comparison of the action of transient and continuous PTH on primary osteoblast cultures expressing differentiation stage-specific GFP. *J Bone Miner Res* 2005;20:5–14.
  45. Bignon A, Chouteau J, Chevalier J, Fantozzi G, Carret JP, Chavassieux P, Boivin G, Melin M, Hartmann D. Effect of micro- and macroporosity of bone substitutes on their mechanical properties and cellular response. *J Mater Sci Mater Med* 2003;14:1089–1097.
  46. Van Hoof VO, De Broe ME. Interpretation and clinical significance of alkaline phosphatase isoenzyme patterns. *Crit Rev Clin Lab Sci* 1994;31:197–293.
  47. Gomez B Jr, Ardakani S, Ju J, Jenkins D, Cerelli MJ, Daniloff GY, Kung VT. Monoclonal antibody assay for measuring bone-specific alkaline phosphatase activity in serum. *Clin Chem* 1995;41: 1560–1566.
  48. Liu XH, Li XM, Fan YB, Zhang GP, Li DM, Dong W, Sha ZY, Yu XG, Feng QL, Cui FZ, Watari F. Repairing goat tibia segmental bone defect using scaffold cultured with mesenchymal stem cells. *J Biomed Mater Res B* 2010;94:44–52.
  49. Havill LM, Rogers J, Cox LA, Mahaney MC. QTL with pleiotropic effects on serum levels of bone-specific alkaline phosphatase and osteocalcin maps to the baboon ortholog of human chromosome 6p23-21.3. *J Bone Miner Res* 2006;21:1888–1896.
  50. Qin XZ, Wergedal JE, Rehage M, Tran K, Newton J, Lam P, Baylink DJ, Mohan S. Pregnancy-associated plasma protein-A increases osteoblast proliferation *in vitro* and bone formation *in vivo*. *Endocrinology* 2006;147:5653–5661.
  51. Li XM, Van Blitterswijk CA, Feng QL, Cui FZ, Watari F. The effect of calcium phosphate microstructure on bone-related cells *in vitro*. *Biomaterials* 2008;29:3306–3316.
  52. Li XM, Feng QL, Wang WJ, Cui FZ. Chemical characteristics and cytocompatibility of collagen-based scaffold reinforced by chitin fibers for bone tissue engineering. *J Biomed Mater Res B* 2006; 77:219–226.
  53. Tu XL, Joeng KS, Nakayama KI, Nakayama K, Rajagopal J, Carroll TJ, McMahon AP, Long FX. Noncanonical Wnt signaling through G protein-linked PKC delta activation promotes bone formation. *Dev Cell* 2007;12:113–127.
  54. Hing KA. Bioceramic bone graft substitutes: Influence of porosity and chemistry. *Int J Appl Ceramic Technol* 2005;2: 184–199.
  55. Li XM, Fan YB, Watari F. Current investigations into carbon nanotubes for biomedical application. *Biomed Mater* 2010;5: 022001.
  56. Habibovic P, Yuan HP, Van den Doel M, Sees TM, Van Blitterswijk CA, De Groot K. Relevance of osteoinductive biomaterials in critical-sized orthotopic defect. *J Orthop Res* 2006;24:867–876.
  57. Ripamonti U, Van den Heever B, Van Wyk J. Expression of the osteogenic phenotype in porous hydroxyapatite implanted extraskeletally in baboons. *Matrix* 1993;13:491–502.
  58. Magan A, Ripamonti U. Geometry of porous hydroxyapatite implants influences osteogenesis in baboons (*Papio ursinus*). *J Craniofac Surg* 1996;7:71–78.
  59. Kuboki Y, Takita H, Kobayashi D, Tsuruga E, Inoue M, Murata M, Nagai N, Dohi Y, Ohgushi H. BMP-induced osteogenesis on the surface of hydroxyapatite with geometrically feasible and nonfeasible structures: Topology of osteogenesis. *J Biomed Mater Res* 1998;39:190–199.